

Visual and X-ray Inspection Characteristics of Eutectic and Lead Free Assemblies

R. Ghaffarian, Ph.D.

Jet Propulsion Laboratory, California Institute of
Technology, Pasadena, CA

Reza.Ghaffarian@JPL.NASA.Gov, (818) 354-2059

ABSTRACT

For high reliability applications, visual inspection has been the key technique for most conventional electronic package assemblies. Now, the use of x-ray technique has become an additional inspection requirement for quality control and detection of unique defects due to manufacturing of advanced electronic array packages such as ball grid array (BGAs) and chip scale packages (CSPs).

Lead-free and lead based assemblies with conventional package, BGA, and CGA (ceramic column grid) were built for inspection by optical and X-ray before and at intervals during thermal cycling with different levels of damage/cracking. Two different 2D real time x-rays were used. The optical images for leaded and leadless assemblies as well those taken for outer rows of area arrays were compared for several solder compositions. These were compared to those inspected by x-ray to understand ability of x-ray for detection of damage/cracking due to thermal cycles. Optical, scanning electron microscopy (SEM), and X-ray photomicrographs for various assemblies were also presented.

Key Words: Inspection, x-ray, ceramic column grid array, CCGA, CGA, solder joint, thermal cycle, lead free, Pb free

INTRODUCTION

BGAs and CSPs (chip scale packages) are now widely used for many electronic applications including portable and telecommunication products. System in a package (SIP) development and use of 3D stack using dices or packages are the most recent response to increasing demand for integration of different functions into one unit to reduce size and cost and improve functionality¹.

The BGA version has now started to be implemented for high reliability applications with unique requirements. The BGA version of the area array package, introduced in late '80's and implemented with great caution in early '90's, was further evolved in the mid '90's to the CSP with a much finer pitch. Now, distinguishing between size and pitch has become difficult for the array versions. These are all now categorized as area array packages in order to be able to distinguish them from the flip chip bare die category. Bare dies have been around for a longer time, but their associated issues- including known good die and difficulty in direct

attachment to printed wiring boards (PWB)- have limited wide implementation for decades. New promising approaches including application of no-flow underfill and use of one station for underfilling and die placement may ease throughput issue and cost².

The CSP definition has evolved as the technology has matured and refers to a package with 0.8 mm pitch and lower, now as low as 0.4 mm pitch. Fine pitch packages, especially those with pitches less than 0.8 mm, and having high I/Os may require the use of costly microvia PWBs. Also, they may perform poorly when they are assembled onto boards.

Extensive work has been carried out by the JPL consortia in understanding technology implementation issues of area array packages for high reliability applications. These included issues with process optimization, assembly reliability characterization, and use of inspection tools including X-ray and optical microscopy for quality control and damage detection due to environmental exposures. Lessons learned by the team have been continuously published³⁻⁵. A Book recently published also includes chapters related to this subject⁴⁻⁶.

Stacking dice/packages are introduced in order to avoid reducing the array pitch and therefore associated issues with stringent requirements for PWBs and routing as well as minimizing assembly defects. The first SIP used CSPs and included two stacks of flash and SRAM die in a single package. Also known as multi chip package (MCP), it has now been recently released in a four die format and may include two flash memories, a fast-cycle-RAM (FCRAM), and an SRAM. The 3D package also become available, stacking to six packages is reported recently⁹.

The BGA version of advanced electronic packages including the flip chip die version (FCBGA) now started to be more widely implemented for high reliability applications with unique requirements. BGAs are known to have excellent process robustness generating less manufacturing defect when are compared to their leaded counterparts. They are, however, more prone to solder joint failures than QFPs because of the attachment with rigid balls. It is shown that most plastic parts when attached on polymer printed circuit board have sufficient reliability with reduced values for their ceramic versions.

Delay in full implementation of the advanced area array packages for high reliability applications, especially space, are mainly due to inability to visually inspect for manufacturing quality and lack of defect detectability, e.g., opens by nondestructive X-ray systems. With FCBGA and 3D and SIP systems, nondestructive evaluation even become more critical.

With industry moving towards implementation of lead free solder attachment, the inspection become an issue even for conventional packages. The wetting angle and appearance

of many of the lead free solders are different and do not have the shininess and small wettability angle of eutectic Sn/Pb solder. This means that for the visible solder joints, new criteria as well as training of QA personnel are needed. This is even become more complicated for area array, SIP, and stack assemblies with multiple overlapping and hidden joints.

The purpose of this paper is to address some aspect of the inspection challenges introduced by the progress of advanced packages. It will discuss the key advantages/disadvantages of optical and X-ray inspections especially for BGA/CGA assemblies. Then, it will provide optical inspection performed for conventional eutectic and lead free packages with different solder materials. Effect of thermal cycling on CSP leadless package with detectable eutectic solder joint will be shown. Finally, optical and x-ray inspections performed for numerous package assemblies with different levels of damage/cracking due to thermal cycling are also presented.

OPTICAL AND X-RAY INSPECTION

Optical Inspection

For high reliability electronic applications, traditionally visual inspection is performed by Quality Assurance Personnel at various package and assembly build steps. Solder joints are inspected and either accepted or rejected based on specific sets of requirements. Further assurance is gained by subsequent short-time environmental exposures including thermal cycles, vibration, and mechanical shock. These screening tests also allow detection of anomalies due to workmanship defects or design flaws at system level. For space application, generally 100% visual inspection is performed at prepackage prior to its closure (precap) and after assembly.

Visual inspection and automatic optical inspection (AOI), while it has been very effective for standard electronics, it may become limited for extremely small dense electronics. The optical tools provide some usefulness for area array packages, but no value for hidden ball/column arrays under the package. SEM and other advanced magnification tools can be used for inspection of tiny packages. Cost, sample size, and potential damage due to electrostatic discharge (ESD) limits the wider usages of SEM technique.

3-D portable optical microscope with improvement in depth-of-field now available that may ease some of the above issues. Representative photos taken by this technique are included in this paper.

X-ray and C-SAM Inspection

For area array packages with hidden solder joints, in addition to process control during manufacturing, nondestructive techniques such as x-ray are needed to determine the integrity of an attachment. During manufacturing process, the 3D laser scanning system has been used to determine solder paste characteristics as a

process control for BGAs/CSPs. Laser scanning can inspect solder paste height and volume, therefore solder paste application uniformity before package placement. By inspecting these attributes, solder print process characteristics such as slumping, scooping or peaks can be identified and controlled.

The inspection system's ability to identify, measure, and analyze defect data after assembly is also critical. Inspection of solder joint integrity of BGAs are important but cannot be effectively performed by visual inspection. Inspection of fine internal structures of microelectronics assemblies, the alignment of hidden interconnects, bridge and voids in BGA assemblies can be carried out using real time X-ray techniques. Internal package delamination, however, cannot be detected by x-ray and other tools such as cross-section acoustic microscopy (C-SAM) is needed.

X-ray transmission radiography is an inspection technique in which x radiation is passed through a specimen to produce a shadow image of its internal structure. Placing the specimen close to the x-ray source enables image magnification, which permits inspection of fine details. Magnifications of greater than 100sX are now obtainable from commercially available equipment.

Visual and X-ray for Defect Detection

Table 1, summarizes some general solder joint defects and compares qualitative accuracy of x-ray and visual inspection. X-ray inspection is excellent for detecting hidden features such as void as well as geometric measurement. However, it is apparent that for some of the unique and most critical defect such as dewetting, crack, cold solder, and disturb solder visual inspection is far superior to x-ray detection. For this reason, both optical and x-ray systems were used to characterized solder joint features of lead free and leaded based assemblies. In addition, investigation was performed to evaluate limitation of x-ray systems for detecting damage/cracking and hidden solder joints. Ideally, a combination of various inspection techniques may be required to be performed in order to assure quality at package and system levels.

INSPECTION TEST RESULTS

Extensive inspection information and photomicrographs at different environmental test intervals for Sn/Pb have been gathered during many years of investigation. Data for lead free presented here, however, is limited to mostly after assembly and with a very limited environmental exposure.

Numerous assemblies were inspected visually prior to environment exposure to document solder joint features prior to environmental tests. Assemblies included both conventional leaded and leadless package as well as CSP leadless packages. In addition, inspection data are provided for a ceramic column grid array with optical and x-ray inspection photomicrographs after assembly and thermal cycles. Both optical and X-ray techniques were used to determine the effectiveness of these techniques on revealing

crack/damage due to thermal cycling. Inspection results for the following assemblies are included:

- 1- Conventional leadless ceramic package with 28 I/Os, 1.27 mm pitch, use Sn/Pb solder, inspection and cross-section after thermal cycles
- 2- CSP leadless package, 46 I/Os, 0.5mm, Sn/Pb solder, inspection and cross-section after thermal cycles
- 3- Conventional J-lead and QFP, BGA, four lead-free solders, optical photos after assembly
- 4- SEM photomicrographs of intermetallic formation after reflow for a lead free solder
- 5- Ceramic column grid array (CGA), 560 I/Os, Sn/Pb solder, inspection after thermal cycles

OPTICAL INSPECTION

Conventional Leadless Package, 28 I/O, 1.27mm pitch

For leaded and leadless package solder joints, the author has performed visual inspection at different magnifications to correlate damage rankings to those revealed by cross-sectioning¹⁰⁻¹¹. Numerous leaded and leadless packages were subjected to thermal cycling, removed at intervals, inspected visually and by scanning electron microscopy (SEM), and results were correlated to cross-sectioning images. An example of such correlation for a ceramic leadless package with 28 I/Os is shown in Figure 1.

Generally, good correlations were found between visual and cross-section rankings for cracks to 100% opening. Assemblies were subjected to a cycle ranging from -55 to 100°C with 4.2 hours per cycle. This figure includes non-destructive images and visual ranks of solder joint cracking to 652 cycles and cross-section images of the same assembly at 652 cycles.

CSP Leadless Package, 46 I/O, 0.5 mm Pitch

The bottom leadless package is a peripheral package for replacing the thin small outline package (TSOP) for DRAM applications. This package uses custom-designed lead frame with the wire bond interconnection at the chip level. A package with 46 I/O was subjected to numerous thermal cycles to determine their cycles-to-failure and their failure mechanisms. Behavior and failure mechanism for those subjected to random vibration discussed in another paper¹².

Figure 2 shows significant damage introduced during thermal cycling in the range of -30 to 100°C, SEM photo and cross-sectioning after 1,500 cycles. Visual inspection could reveal the outer damage and therefore provide an indication of internal damage. Outer and internal damage, however, were less apparent for those subjected to random vibration¹².

Leaded Package with Lead Free Solder Joint

In an investigation¹³ that is underway at Jet Propulsion Laboratory, investigators have selected four lead-free solders for initial screening and subsequent down selection, rebuild, and environmental testing. The four alloys were:

- 1- Sn96.5Ag3.5 (eutectic) with 221 melting point, melting like a metal, it has good wetting characteristics, and better strength than Sn/Pb, even though it may show weakness at interface.
- 2- Sn95.5Ag3.8Cu0.7, this alloy recommended by NEMI and used by Japanese and European. With a melting temperature of 217-218 with no plastic range. Formation of Cu₆Sn₅ and especially Ag₃Sn plates, may have positive or negative effect depending on its level (see below).
- 3- SN96.2Ag2.5Cu0.8Snb0.5 (Castin®) with melting point of 217-218, improve thermal fatigue and Sb reduces melting point even though it may show toxicity at higher temp.
- 4- Sn77.2In20Ag2.8 (Indalloy) with a large plastic melting range of 175-187°C, is comparable melting to Sn/Pb, good ductility and creep resistance. It is costly, and its 118°C eutectic point may deteriorate mechanical properties of solder joint.

Figure 3, compares optical photos of solder joint for a J-lead plastic package for the above four lead-free alloy composition as well as a J-lead ceramic package attached with Sn/Pb solder. Figure 4, shows photos of the four lead-free solders for a QFP plastic package. Figure 5, compares ball grid array with S/Pb and lead-free solder attachment. Figure 6 give x-ray representative photos of BGAs with lead-free solder.

You may note that Sn/Pb solder is shiny with an excellent wetting. The only lead-free solder joint that come close to Sn/Pb feature is Sn96.5Ag3.5, a eutectic solder. All lead-free solders show appearance of a graininess and lack of good wettability.

1. Sn96.5Ag3.5 (eutectic), it is grainy, but much better than other lead-free compositions
2. Sn95.5Ag3.8Cu0.7, showed graininess, rugged fillet formation, and voids
3. SN96.2Ag2.5Cu0.8Snb0.5 (Castin®), it is very similar to #2, in some case better appearance quality than #2
4. Sn77.2In20Ag2.8 (Indalloy 227), rougher than others possibly due to Indium, also lacks good wetting

REASONS FOR LEAD FREE OPTICAL DULL APPEARANCE

The above characteristics of lead-free different from Sn/Pb make visual inspection and especially automatic optical inspection (AOI) a challenge. The reasons for the lead-free solder joint appearance are as follows:

- 1- Lead-free solder joint surfaces tend toward dull, matte, rough, and grainy finish contrary to shiny surface for Sn/Pb. This is generally because lead-free is non-eutectic composition. After reflow, it drops in temperature slow and non-uniform because of having a "plastic" region. For example, Indalloy 227, has a melting temperature range from 175 to 187°C, solidus-to-liquidus temperature range. Because of this, metal composition starts to solidify non-uniformly in order

liquid and solid coexist in equilibrium as defined by their phase diagram. This is the source of dull surface which depends on composition and its closeness to eutectic or pure alloy composition. In contrast, Sn/Pb which is a eutectic alloy melts at a constant temperature like a pure metal.

- 2- Fillet shape of lead-free joints which is a function of wettability angle are generally uneven, therefore producing inconsistency in appearance and requirement for a unique inspection criteria. Fillet shape depends on many variables including wettability angle of solder to lead surface finish and pad, flux selection, and reflow temperature. Lead-free surface tension is stronger than Sn/Pb, therefore, less prone to spreading with appearance of lack of wetting.
- 3- Reflectivity depends on solder surface finish and therefore time solder to solidify. Good reflectivity will be observed when Sn/Pb or eutectic composition of lead-free alloy is used.

Lead Free Intermetallic Formation after Reflow

The effect of lead free paste print parameters for various BGA and CSPs were narrowed in a previous study¹⁴. After paste print, the boards with lead-free solder (Sn95.5Ag3.8Cu0.7) were subjected to numerous reflow to understand the effect of a 244°C reflow temperature on integrity of boards as well as microvias. Boards with S/Pb were subjected to a 210°C reflow as control. Marginal increase in daisy chain resistance of plated-through-hole (PTH) and microvia was observed. Figure 7 compares lead-free and lead based microstructure over microvia after three reflows. Figure 8 shows details on intermetallic microstructure of lead-free after 3 reflows. Etching and removal of Sn was performed to reveal details of intermetallic formation and growth. Plate like intermetallic of Ag3Sn with extensive penetration into matrix and extending from one side of microvia into another is of interest. These plates could cause initiation of microcrack due to their lack of ductility and therefore cause embrittlement at solder joint interface as well as within solder joint.

CGA Visual Inspection

Figure 9 shows optical photomicrographs of the CGA assembly prior to thermal and after cycling when some signs of damage/cracking was observed by visual inspection. Figure 10 shows SEM photomicrographs and cross-section of the assemblies after cracking due to thermal cycles. As stated previously, 3D optical microscopy and visual inspection are limited to inspection of outer rows of area array assemblies and could be performed only when enough gaps are allowed between the assembled parts. The assemblies after thermal cycles show signs of damage/cracking.

X-RAY INSPECTION

Two different X-ray systems were used for evaluation of various package/assemblies after thermal cycle exposures.

Unique features of these systems as well as results are discussed:

2D X-ray, System 1

A 2D inspection system with a microfocus source and image intensifier as detector, capable of producing offset pseudo 3D features¹⁵. This system was limited to 2D inspections and capability of small sample rotation/tilt. The sample holder was not used since samples were larger than the capability of the sample holder. The transmission x-ray captures everything between the x-ray source and image intensifier. X-rays then emit from the source and travel through the sample. The higher the density of the sample, e.g., columns in CGAs, the fewer x-rays will pass through and be captured by the image intensifier. The x-rays are displayed in a grayscale image, with the lower density, such as voids, areas appearing brighter than the higher density areas. The voltage and current of the x-ray's intensity can be adjusted to reveal features of the most section of sample.

The 2D x-ray systems are very effective in testing single-sided assemblies. With the use of a sample manipulator, oblique view enhances inspection of both single and double-sided assemblies with some loss of magnification due to increase in distance between source and detector. Experience needed in discerning between bottom-side board elements and actual solder and component defects. This can be very difficult or impossible on extremely dense assemblies. As discussed previously, certain solder-related defects such as voids, misalignments, solder shorts, etc. are easily identified by transmission systems. However, even an experienced operator can miss other anomalies such as insufficient solder, open connection, and cold solder.

Figure 11 shows X-ray photomicrograph for assembled CGA after thermal cycle exposure using the 2D X-ray transmission system discussed above for case 1 where parts remained stationary during x-ray exposure. Solder joints could not be detected because of significant x-ray intensity attenuation by CGA column.

2D X-ray, System 2

The second system that was utilized for evaluation is also a 2D x-ray tool with a similar microfocus source intensity and stationary position, but detector had off-axis rotational capability¹⁶. This feature allows oblique generation of x-ray images with a higher magnification and a better intensity resolution since the focal spot remains the same and therefore no loss of magnification. An isocentric manipulator keeps the field of view unchanged when the oblique view mode is used. This feature allows better characterization of some defect features including wettability and voids location in area array packages.

Figure 12 shows x-ray photomicrographs of assembled CGA after thermal cycles using the case 2 X-ray system with an oblique view capability. X-ray images from two views are included. CGA columns having high lead composition (90Pb/10Sn) are much darker than eutectic

solder (37Pb/63Sn) used for attachment to the board. Within lighter solder joints at lower section of column, other lighter zig zag lines, possibly caused by cracking, are apparent. Non-smoothness of patterns may be an indication of solder graininess generally occurs as thermal cycle progress due to solder grain growth.

CONCLUSIONS/RECOMMENDATIONS

Lead-free solder joints generally showed grainy appearance with somewhat lack of wetting when they are compared to Sn/Pb. New inspection criteria for lead-free solder joints and even solder balls in BGAs need to be developed and QA personnel be trained, especially for high reliability applications, where visual/optical inspection often used for acceptance/rejection. AOI also need to be modified to include acceptance criteria for the lead-free features.

Optical inspection along with nondestructive systems with finer feature detectability such as x-ray and C-SAM, become critically important as electronic package/assembly become more complex, feature sizes decrease, and hidden interconnects such as BGAs are used. X-ray systems are significantly improved since a decade ago, however; still they have their limitations. Many features of area array package assembly, e.g., shorts and voids, could be easily detected either by 2D x-ray systems. However, heavy solder joint damage/cracks in a CGA assembly induced by thermal cycles, could only be partially detected by a 2D X-ray system having an oblique view capability.

X-ray features of lead-free solder for plastic packages appear to be the same feature as lead based solder. X-ray systems need to be further developed to meet microelectronic size reduction and complexity as well as distinguish composition of many lead-free solder interconnects. Further investigations are being carried out in order to understand correlation between damage/cracks detected by optical/SEM/cross-sectioning and x-ray systems.

ACKNOWLEDGEMENTS

The research described in this publication is being conducted at the Jet Propulsion Laboratory, California Institute of Technology, under a contract with the National Aeronautics and Space Administration.

The authors would like to acknowledge funding through NASA Electronic Parts and Packaging Program (NEPP). The author would like to acknowledge contribution of Dr. J.K. Bonner, A. Mehta, and K. Evans at JPL and the in-kind contribution of JPL-lead consortia team members. Also, in-kind technical and X-ray test performed by Phoenix X-ray is appreciated.

REFERENCES

1. Ghaffarian, R. "3-D Chip Scale Package", *Chip Scale Packaging for Modern Electronics* (Electrochemical Publications, 2002), chapter 15
2. Zhang, J.J., et al, "An Innovative Underfill Process for High-Speed SMT CSP BGA Flip Chip Assembly", IEEE International Electronics Manufacturing Technology Proceedings, San Jose, July 16-18, 2003
3. Ghaffarian, R., Kim, N., "CSP and BGA Assembly Reliability in a Fast Ramp Rate Thermal Cycle Environment", The Proceedings of Surface Mount International, Chicago, Sept. 30-Oct 4, 2001
4. Ghaffarian, R., "Shock and Thermal Cycling Synergism Effects on Reliability of CBGA Assemblies", 2000 IEEE Aerospace Conference Proceedings, 2000, p327
5. Ghaffarian, R. "Chip Scale Package Issues", *Microelectronics Reliability*, vol 40, p 1157-61
6. Fjelstad, J., Ghaffarian, R., Kim, YG., *Chip Scale Packaging for Modern Electronics* (Electrochemical Publications, 2002)
7. Ghaffarian, R., "Chip Scale Package Assembly Reliability", Chapter 23rd in *Area Array Interconnect Handbook* (Kluwer Academic Publishers, edited by Karl Puttlitz, Paul Totta, 2002)
8. Ghaffarian, R., "BGA Assembly Reliability", Chapter 20, *Area Array Packaging Handbook* (McGraw-Hill Publisher, Ken Gilleo, Editor)
9. Demmin, J.C., et al, "Stacked Chip Scale Packages: Manufacturing Issues, Reliability Results, and Cost Analysis", IEEE International Electronics Manufacturing Technology Proceedings, San Jose, July 16-18, 2003
10. Ghaffarian, R., "The Interplay of Surface Mount Solder Joint Quality and Reliability of Low Volume SMAs," NEPCON WEST Proceeding, Feb. 25-29, 1996, Anaheim, CA
11. Ghaffarian, R., "Solder-Joint Quality with Low-Volume PCB Processing," *SMT Magazine*, July 1996
12. Ghaffarian, R., Kim, N., "Vibration of CSP Assemblies with and without Underfill", The Proceedings of Surface Mount International, Chicago, Sept. 21-25, 2003
13. Bonner, J.K., Del Castillio, L., Mehta, A., "Hi-Rel Lead-Free Printed Wiring Assembly", The Proceedings of Surface Mount International, Chicago, Sept. 22-26, 2002, page 453
14. RamKumar, M., et al, Ghaffarian, R., "Reliability of and Paste Process Optimization of Eutectic and Lead-Free for Mixed Packaging", The Proceedings of Surface Mount International, Chicago, Sept. 22-26, 2002, page 795
15. <http://www.feinfocus.de/>
16. <http://www.microfocus-x-ray.com>

Table 1 Key solder defect types and ability to detect visible joints

VISIBLE FEATURES	X-ray Inspection	Visual Inspection
Stress marks, Cracks	0	+++
Open Contacts	0	++
Cold/Disturb Joint	0	+++
Dull Solder	0	+++
Flux residue/Contamination	0	+++
Porosity and Voids in Solder	+++	0
Solder thickness/volume	+++	0
Heel/Toe Side Fillets	+++	++
Solder balls	+++	++
Solder Bridge	+++	++

+++ Excellent detection
 ++ Good detection
 0 Poor or unacceptable

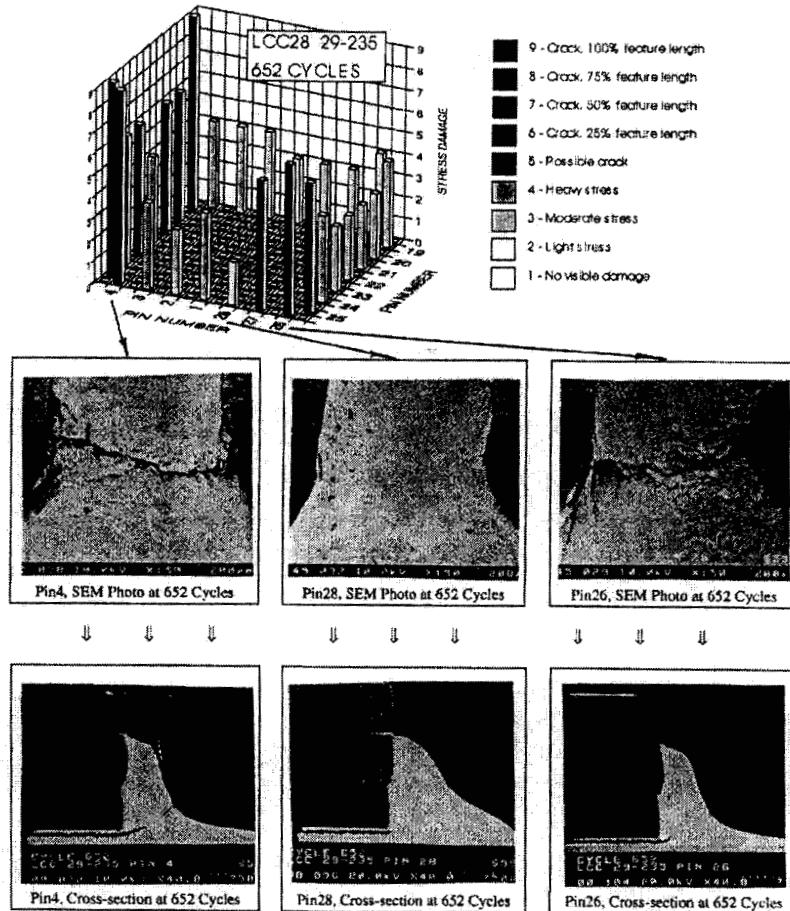


Figure 1 Correlation between visual inspection for damage (crack) progress with thermal cycling and destructive cross-sectional microphotographs. Ceramic Leadless package, 28 castellations, 1.27 mm pitch.

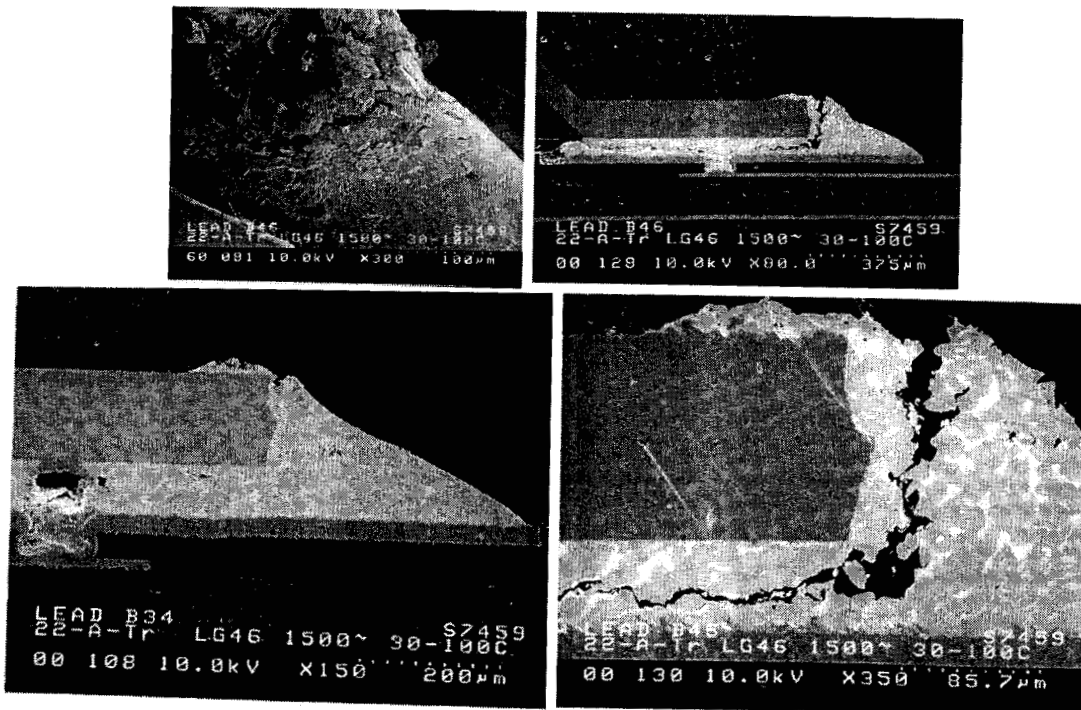


Figure 2 SEM photomicrographs of a 46 I/O leadless package, 0.5 mm pitch, before and after cross-sectioning. Visual damage correlates with internal cross-section micrographs.

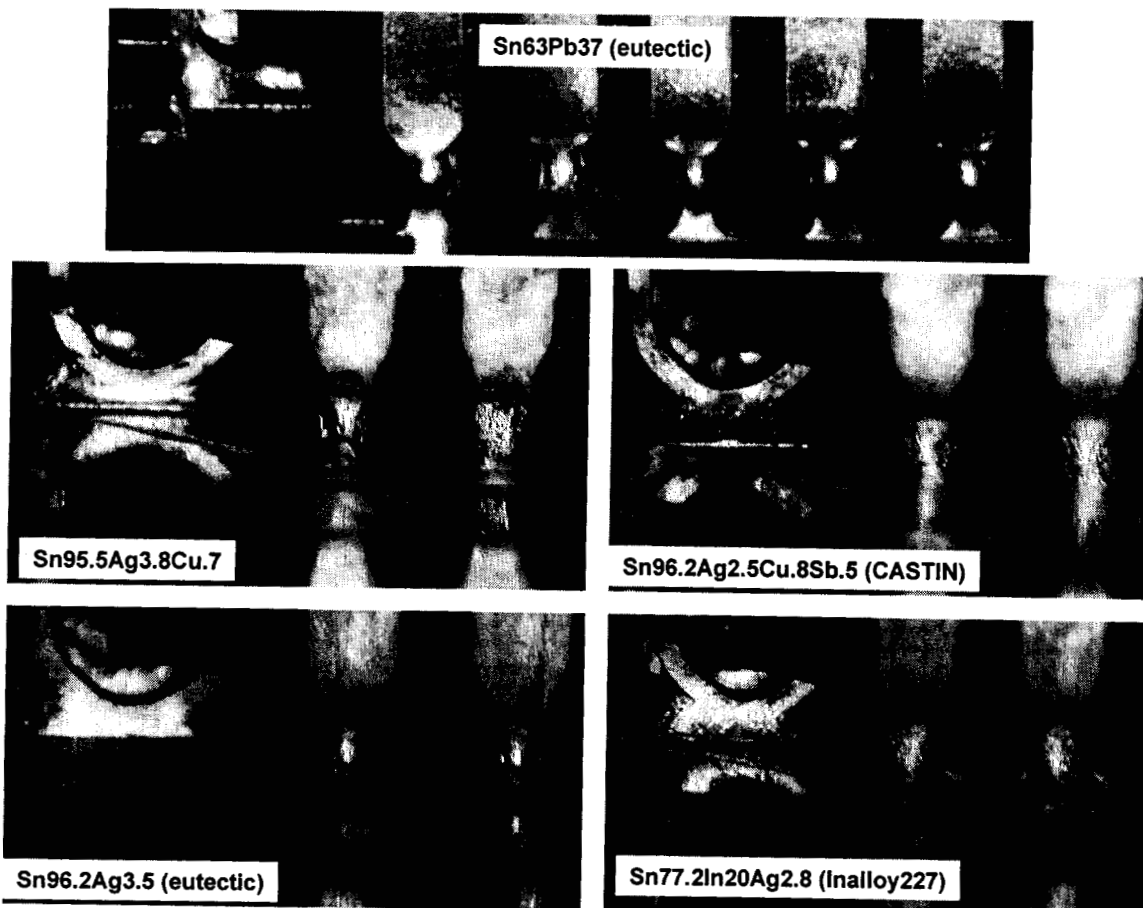


Figure 3 Optical photos of J-lead packages assembled with Sn/Pb solder and four lead-free solders. Note differences in solder wetting angle and appearance. The lead free eutectic solder (Sn96.2Ag3.5) has closer appearance to lead based solder.

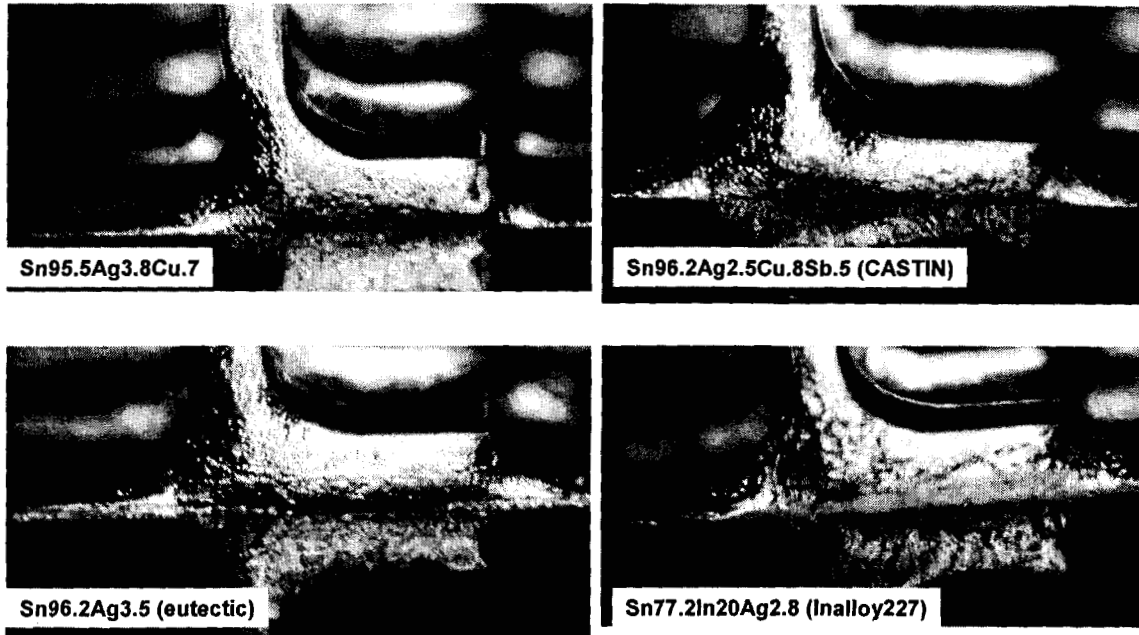


Figure 4 Optical Micrograph of QFP packages assembled with four different lead free solders. Note differences in solder wetting angle and their graininess appearance.

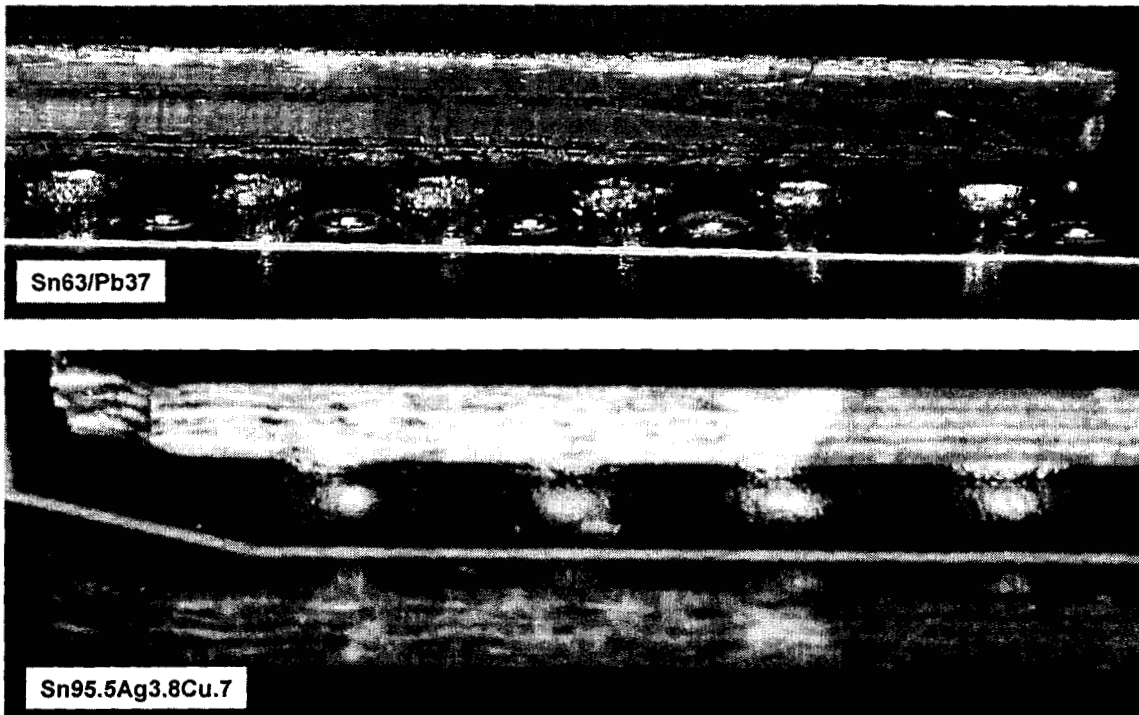


Figure 5 Optical Micrograph of BGA outer row solder balls of eutectic and lead free solders

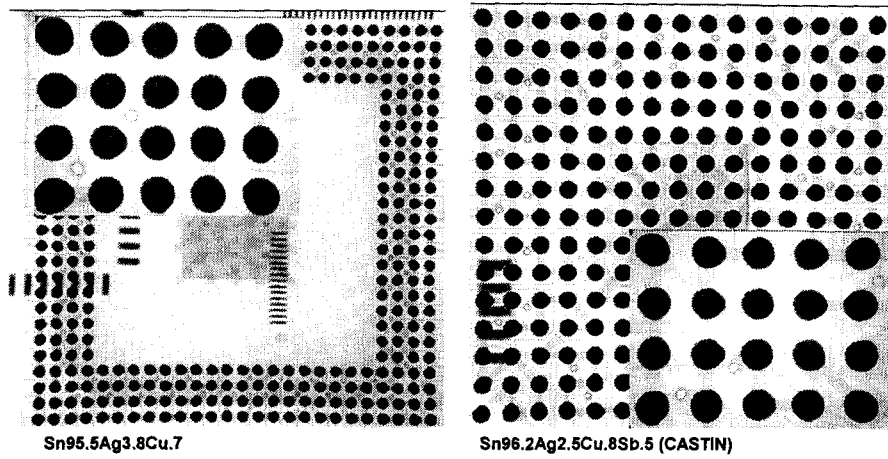


Figure 6 X-ray photographs of BGA assemblies with lead free solder.

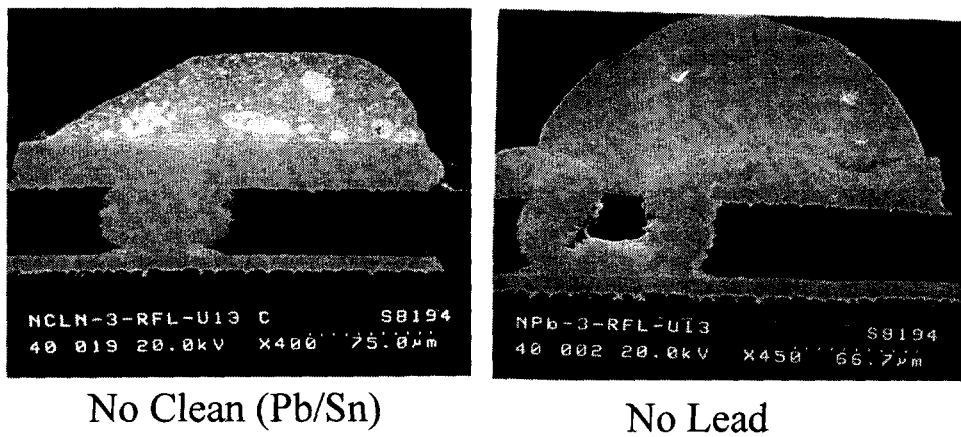


Figure 7 SEM photomicrograph of Sn/Pb and lead-free (no lead) of assemblies underwent 3 reflows

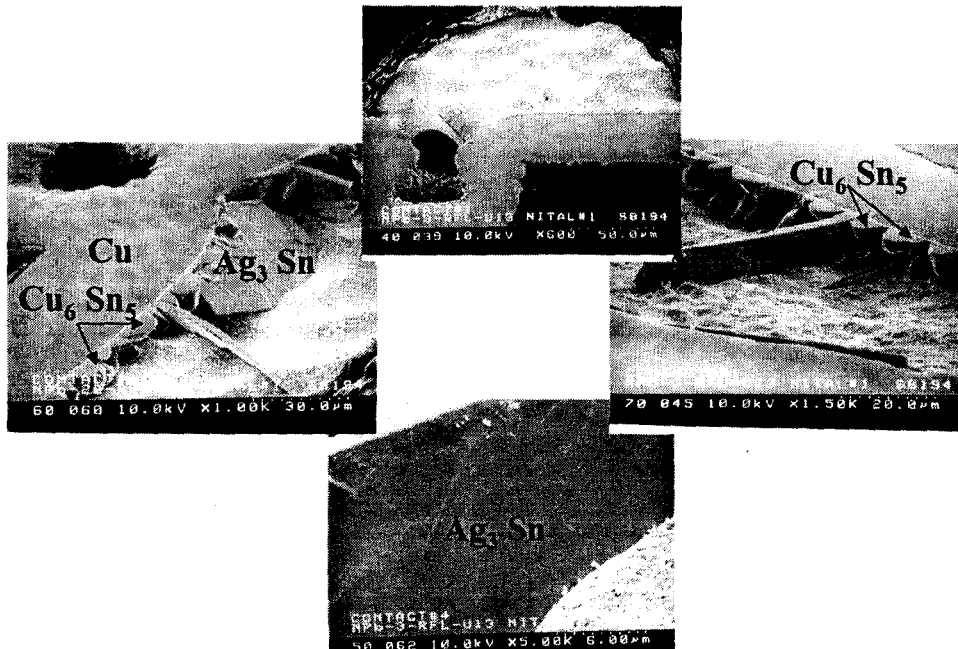


Figure 8 SEM photomicrograph of intermetallic in lead free solder after reflow. Note large platelike after 3 solder reflows

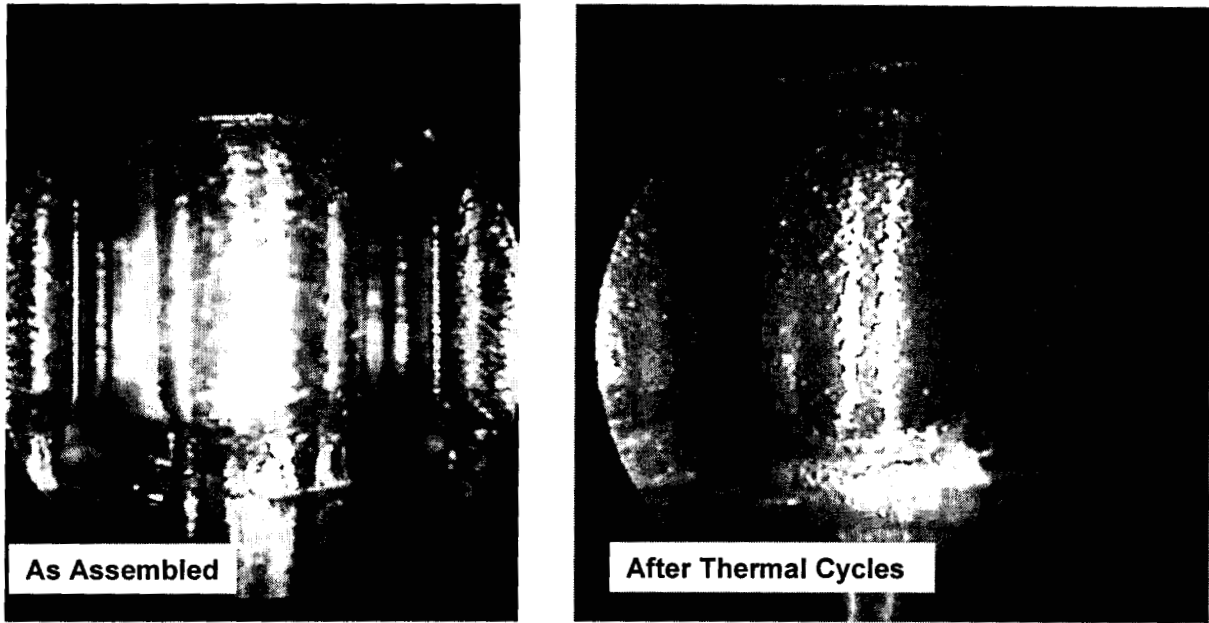


Figure 9 3D optical photomicrographs of CGA before and after damage/crack observation

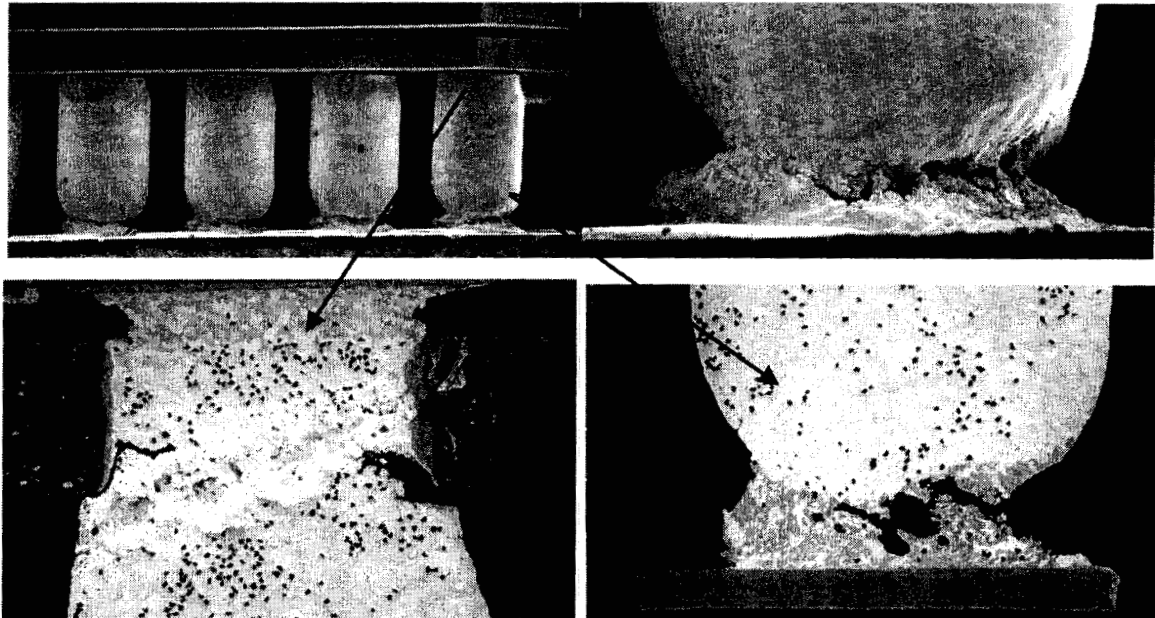


Figure 10 SEM photomicrographs and cross-section of CGA after damage/crack observation due to thermal cycling

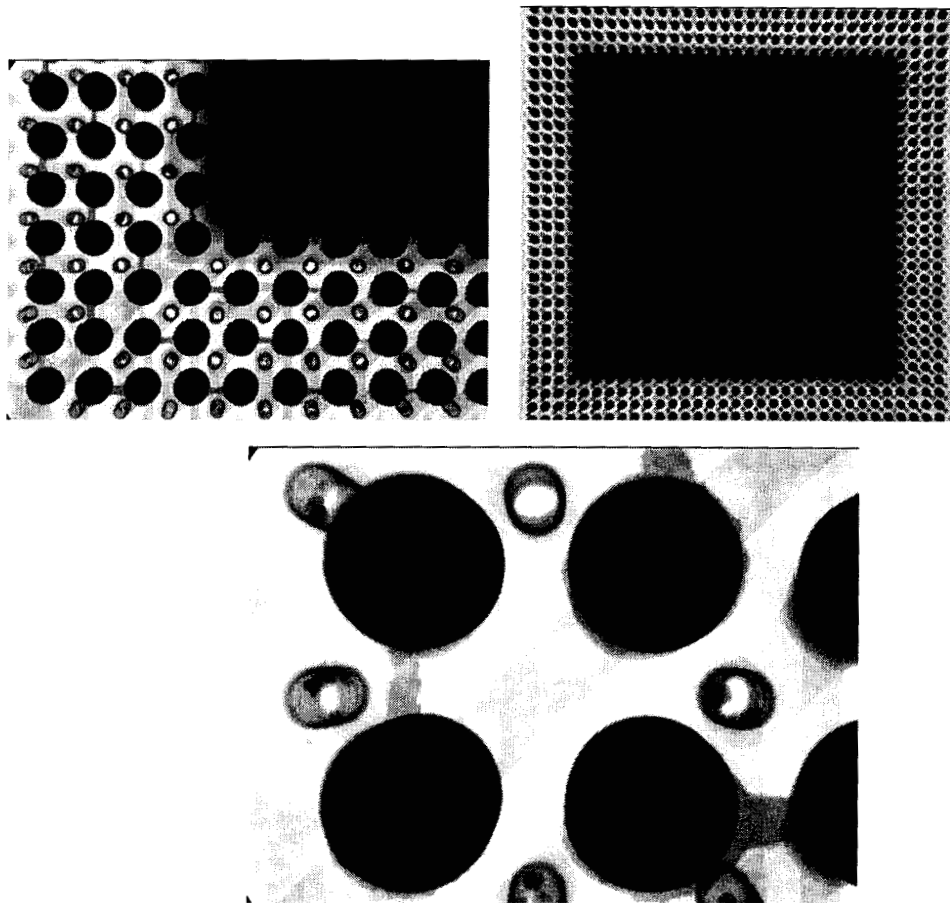


Figure 11 2D X-ray inspection of CGA assembly after thermal cycles. Damage/cracks observed visually and by SEM and cross-sectioning are not detectable

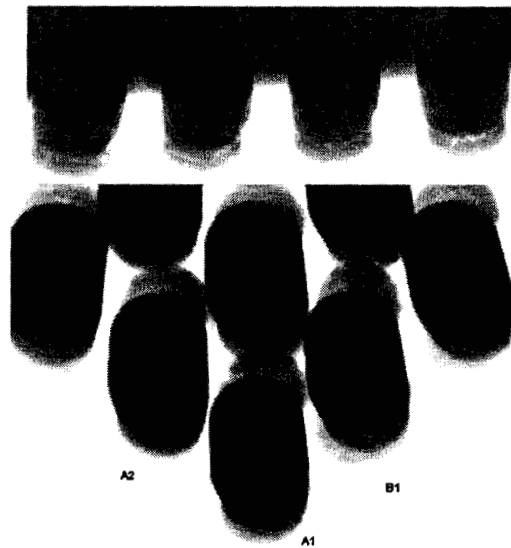


Figure 12 X-ray photomicrographs of CGA using a 2D X-ray system with oblique detector at two angles. Signs of cracking/damage is somewhat apparent.